

Magnetic features near filled impurity band in diluted magnetic semiconductorsVan-Nham Phan^{1,2,*} and Huu-Nha Nguyen³¹*Institute of Research and Development, Duy Tan University, Da Nang 550000, Vietnam*²*Faculty of Natural Sciences, Duy Tan University, Da Nang 550000, Vietnam*³*Department of Theoretical Physics, VNUHCM-University of Science, Ho Chi Minh City 700000, Vietnam*

(Received 5 February 2020; revised 23 July 2020; accepted 30 August 2020; published 14 September 2020)

The antiferromagnetic-ferromagnetic competition in a diluted magnetic semiconductor is discussed. In a virtual-crystal approximation, the active magnetic ions in the system are assumed to distribute homogeneously, and the quantum magnetic correlations are described in the Kondo lattice model involving local disorder. In the framework of the dynamical mean-field theory, we deliver the signatures of the static magnetic susceptibility function and the B_{1g} channel Raman response adapting to the model. At low temperatures, one finds the antiferromagnetic instability against the ferromagnetic state when the impurity band is nearly filled. For a completely filled impurity band system, the antiferromagnetic state is stabilized in the case of sufficiently large magnetic exchanges. The effect of the thermal fluctuations on the phase competition is also discussed. Analyzing the B_{1g} channel Raman spectrum attributes a competition between the short-range magnetic order and the short-wavelength excitation in the filled impurity band paramagnetic state.

DOI: [10.1103/PhysRevB.102.125202](https://doi.org/10.1103/PhysRevB.102.125202)**I. INTRODUCTION**

Due to the essential properties for applications in future spintronics, the signature of magnetic instabilities in diluted magnetic semiconductors (DMSs) has become a special issue attracting much interest recently [1,2]. Once magnetic elements (e.g., Mn) are doped in a semiconducting host (e.g., GaAs), their $3d$ levels simultaneously induce localized magnetic moments and form an impurity band [3]. It has been widely accepted that the band structure of the system involves a valance-hole band of the host semiconductor and localized impurity bands of the magnetic doped ion, which induce the exchange interaction mediating the magnetic properties in the system based on the Zener kinetic-exchange or p - d exchange model [1,2,4–6]. Increasing the magnetic coupling enlarges the energy gap that separates the impurity band and the valance band [7,8]. In the case of the strong-coupling limit, the p - d exchange model might reduce to the double-exchange model [2], otherwise it becomes equivalent to the Ruderman-Kittel-Kasuya-Yosida (RKKY) picture for small magnetic coupling [5]. In this feature, once the impurity band is filled or nearly filled, a large magnetic exchange might forbid the ferromagnetic (FM) configuration due to Pauli's principle. Instead, the antiferromagnetic (AFM) state is favored due to the development of a virtual hopping process [9]. In this case, the ground state of the system is AFM and the band energy of the FM state is lower than that of the AFM stability [9–11]. So far, the magnetic instability in DMSs has

been mainly considered when the impurity band is not fully filled, and the system stabilizes in the FM state [4,7,12]. In the meanwhile, AFM materials have shown many advantages in spintronic applications. Examining the AFM state in DMSs is, therefore, extremely necessary [13]. Although the AFM state has been considered both in theory and in experiments, typically in $\text{Ga}_{1-x}\text{Mn}_x\text{As}$ and $\text{Zn}_{1-x}\text{Mn}_x\text{Te}$ [5], in GaN doped with 5% Mn and Co [14], or most recently in (Ga,Mn)As [15], signatures of the AFM state induced by the p - d exchange in DMSs once the impurity band is filled or nearly filled are not well understood. Considering the competition of the AFM and FM states and especially features of their transition from the paramagnetic (PM) state in a unique theoretical framework is thus enormously worthwhile.

To understand the characteristics of the PM-FM transition in DMSs, a formation of short-range magnetic order (SRMO) of bound magnetic polarons has been proposed [12,16,17]. However, that feature has not been used to explain a mechanism of the PM-AFM transition in the materials. To describe the signature of the PM-AFM transition in undoped AFM materials, one has proposed a short-wavelength (two-magnon) excitation mechanism [18] that has been specified theoretically in the t - J model using the finite-temperature diagonalization method [19]. In our work, short-wavelength excitation (SWLE) is considered to address a magnetic bound state to describe the PM-AFM transition in DMSs. The phase diagram of the magnetic transitions in the systems is constructed from the typical property of the static magnetic susceptibility; divergence of the susceptibility indicates an instability point of the order state. Moreover, in a signature of the Raman scattering spectrum, one might point out the magnetic bound state possibility existing in the PM state. Indeed, the Raman response has proven to be an effective tool for studying complex phase structures and especially in

*Present address: Institute of Research and Development, Duy Tan University, Da Nang 550000, Vietnam; Faculty of Natural Sciences, Duy Tan University, Da Nang 550000, Vietnam; phanvannham@duytan.edu.vn

addressing the spin-disorder, magnetic polaron, and FM states in low-carrier density magnetic systems [16,20]. Focusing on DMSs, the Raman scattering spectrum has probed the magnetic bound state in $\text{Cd}_{1-x}\text{Mn}_x\text{Te}$, by using the bound magnetic polaron theory [21,22].

One of the most prevailing methods in dealing with strongly correlated electron systems is the dynamical mean-field theory (DMFT), which gives an exact solution in the limit of infinite-dimensional space [23]. The DMFT has been widely used in studying the magnetic properties in DMSs and similar systems [7,8,17,24]. Based on the DMFT, the ground state of the AFM-FM competition in the double-exchange model has been intensively inspected [25]. In the infinite-dimensional limit, DMFT also provides a simple way to analyze the Raman B_{1g} channel spectrum and the static magnetic susceptibility function potentially addressing some anomalous properties in strongly correlated electron systems [26]. In the present work, the DMFT is applied to the Kondo lattice model to investigate the magnetic properties of DMSs. In general, the Kondo lattice model is used to describe a system in which local moments homogeneously reside at each site of the lattice. However, to model and explain the magnetic properties in DMSs, we assume that the active Mn ions are distributed homogeneously in the system in a virtual-crystal approximation [6]. In this signification, the magnetic moments reside on all lattice sites, or the magnetic exchange potential due to the Mn impurities has the periodicity of the host crystal. The Kondo lattice model, therefore, can be applicable to describe the magnetic properties of the diluted magnetic system [6]. In this sense, for instance, a carrier feels a potential with mean strength approaching xJ per GaAs unit cell, for Mn concentration x and magnetic coupling J [7].

The paper is organized as follows. In the next section, we briefly describe the essential Hamiltonian based on the feature of the Kondo lattice model applied for DMSs and its DMFT solution. A set of self-consistent equations based on the DMFT is used to calculate analytically the static spin susceptibility function. Numerical results for the magnetic phase diagrams and Raman scattering spectrum are discussed in Sec. III. Finally, Sec. IV concludes our work.

II. MODEL AND THEORETICAL METHOD

Suppose the doped magnetic ions in the DMSs act as an acceptor, and the main charge carrier is the hole [5]. We examine the following Hamiltonian in the framework of the Kondo lattice model to describe the magnetic signatures in DMSs:

$$\mathcal{H} = -t \sum_{(i,j)\sigma} c_{i\sigma}^\dagger c_{j\sigma} + 2J \sum_i \alpha_i \mathbf{S}_i \mathbf{s}_i - \sum_i (\mu - U\alpha_i) n_i, \quad (1)$$

where $c_{i\sigma}^\dagger$ and $c_{i\sigma}$ are the creation and annihilation operators for an itinerant carrier with spin σ at lattice site i , respectively. In this representation, the spin and occupation operators of the itinerant carriers at site i , respectively, read $\mathbf{s}_i = \sum_{\sigma\sigma'} c_{i\sigma}^\dagger \boldsymbol{\sigma}_{\sigma\sigma'} c_{i\sigma'}$ ($\boldsymbol{\sigma}$ are the Pauli matrices) and $n_i = \sum_{\sigma} c_{i\sigma}^\dagger c_{i\sigma}$. The first term in Eq. (1) indicates carrier hopping between the nearest neighbor, while the second one expresses the Hund magnetic coupling between spins of itinerant carriers and the impurity moment at lattice site i (\mathbf{S}_i). In our

work, \mathbf{S}_i is treated quantum mechanically. Indeed, within the DMFT calculation adapted for double-exchange-like models, the self-energy of the single-particle Green function does not change if the local spin is considered either in the classical or in the quantum case [27,28]. Moreover, the essential features of magnetic and electronic properties in DMSs do not depend on whether the exchange coupling is of Ising- or Heisenberg-type [8,29]. So, as a simplification, we assume that the magnetic coupling in our model is of Ising-type, i.e., only the z -component of the spins is of interest. In doing so, without loss of generality, the local moment is often chosen to take two values, $S_i^z = \{-1, 1\}$ [17,30]. Finally, in the Hamiltonian (1), μ indicates the chemical potential while U is the magnetic disorder mapping onto the difference in the local potential.

In the Hamiltonian (1), we have included an α variable to indicate whether a lattice site is doped by an active magnetic ion or not. In this sense, we set $\alpha = 1(0)$ to the lattice sites that are occupied (not occupied) by magnetic ions, or there exists (does not exist) spin coupling and magnetic disorder. If x is the doping number of the magnetic ions in DMSs, α satisfies a binary distribution function

$$\mathcal{P}(\alpha) = (1-x)\delta(\alpha) + x\delta(1-\alpha). \quad (2)$$

In general, to address the disorder properly, the on-site energy has to be taken randomly. However, to simplify our calculation, we have used the bimodal distribution for the disorder. It is applicable because the disorder potential U here is included to map onto the difference in the local potential, which splits energetically in favor of the lattice site with and without magnetic doping. The disorder in our work, therefore, is so-called local disorder. It looks like a binary alloy disorder and can be approximately suitable for a lightly doped material [31,32]. In some other works for DMSs, U can be taken to be like the Coulombic potential arising from the magnetic dopant [7,8]. The local disorder is generally site-dependent or spatially inhomogeneous. However, the disorder here has been introduced on average and is a kind of diagonal disorder. Such diagonal disorder has been studied intensively in the literature using the infinite-dimensional DMFT [23,33].

In the present work, the Hamiltonian in Eq. (1) is solved using DMFT. As a nonperturbative local theory, the DMFT solution is exact in the limit of infinite-dimensional space. In DMFT, the mean field is dynamical or time/frequency-dependent, and the temporal quantum fluctuations are thus fully taken into account. In the meanwhile, the spatial fluctuations are ignored [23]. The key point of the DMFT is that the frequency-dependent Green function of itinerant carriers must coincide with one of the effective single impurities embedded in the dynamical mean-field medium [23]. The local Green function of itinerant carriers with spin σ reads

$$G_\sigma(i\omega_l) = \int d\varepsilon \rho(\varepsilon) \frac{1}{i\omega_l - \varepsilon + \mu - \Sigma_\sigma(i\omega_l)}, \quad (3)$$

where $\omega_l = (2l+1)\pi T$ is the Matsubara frequency at temperature T , $\Sigma_\sigma(i\omega_l)$ is the momentum-independent self-energy, and $\rho(\varepsilon) = \exp(-\varepsilon^2)/\sqrt{\pi}$ is the noninteracting density of states of the itinerant carriers in the infinite-dimensional hypercubic lattice. The Green function defined in Eq. (3) must be coincident with that evaluated from the

effective single impurity based on the Hamiltonian (1), i.e.,

$$G_\sigma(i\omega_l) = \sum_s \int d\alpha \mathcal{P}(\alpha) \frac{\Xi_{\alpha s}}{Z_\sigma^{\alpha s}(i\omega_l)}. \quad (4)$$

Here, we have defined $Z_\sigma^{\alpha s}(i\omega_l) = \mathcal{G}_\sigma^{-1}(i\omega_l) - (Js\sigma + U)\alpha$, with $\mathcal{G}_\sigma(i\omega_l)$ the Green function of the effective medium. When calculating the Green function in Eq. (4), the average over the spin configuration has been taken through the weight factors $\Xi_{\alpha s}$ with $s = \{-1, 1\}$ satisfying the normalization condition $\sum_s \int d\alpha \mathcal{P}(\alpha) \Xi_{\alpha s} = 1$. If the local spin is assumed to be classical, the average over the spin configuration can be taken by a Monte Carlo method [34,35].

In the form of the distribution function defined in Eq. (2), one arrives at

$$G_\sigma(i\omega_l) = \sum_{\alpha s} \frac{\Lambda_{\alpha s}}{Z_\sigma^{\alpha s}(i\omega_l)}. \quad (5)$$

Here, α takes two values, $\alpha = \{0, 1\}$, and the weight factors explicitly read $\Lambda_{0s} = 2(1-x) \exp \sum_{l\sigma} \ln[\mathcal{G}_\sigma^{-1}(i\omega_l)/i\omega_l]/Z_{\text{eff}}^0$ and $\Lambda_{1s} = 2x \exp \sum_{l\sigma} \ln\{[\mathcal{G}_\sigma^{-1}(i\omega_l) - (Js\sigma + U)]/i\omega_l\}/Z_{\text{eff}}^1$, where $Z_{\text{eff}}^\alpha = 2 \text{Tr} \exp \sum_{l\sigma} \ln[Z_\sigma^{\alpha s}(i\omega_l)/i\omega_l]$ is the partition function. The local Green function is found self-consistently via the Dyson equation

$$G_\sigma^{-1}(i\omega_l) = \mathcal{G}_\sigma^{-1}(i\omega_l) - \Sigma_\sigma(i\omega_l). \quad (6)$$

Equations (3)–(6) close a set of self-consistent equations that must be solved numerically to evaluate the self-energies $\Sigma_\sigma(i\omega_l)$ and then the itinerant carrier Green function.

To detect the magnetic phase transition, magnetic order parameters such as the magnetizations are often analyzed [25,36]. In the present work, we examine the magnetic instabilities in the signatures of the static magnetic susceptibility of the itinerant carriers, which is defined as [37]

$$\chi(\mathbf{q}) = T^2 \sum_{ijl, \sigma\sigma'} \left. \frac{dG_{ii, \sigma}(i\omega_l)}{dh_{j\sigma'}} \right|_{h_{j\sigma'}=0} \sigma\sigma' e^{-iq(\mathbf{R}_i - \mathbf{R}_j)}. \quad (7)$$

Note here that, in general, the magnitude of the local magnetic moment might be larger than that of the itinerant spins, and the magnetic susceptibility of the local moment should be evaluated to explore the magnetic properties of the system. However, in the model we have assumed that the spin of the itinerant carrier is always parallel to the local spin to optimize the total energy. Considering the order of the local spin and that of the itinerant spin, therefore, is equivalent. In the meanwhile, calculation of the magnetic susceptibility of the itinerant carriers is much simpler than that of the local spins, especially in the DMFT. We therefore refer to the behavior of the spin susceptibility of the itinerant carriers, and it truly addresses the magnetic behaviors of the full system. It is likely that the magnetic features remain unchanged if the local magnetic susceptibility is considered instead. Another way to simplify the numerical calculations is to consider the magnetic properties in the signature of the susceptibility in DMFT that we are familiar with in momentum space. Following the standard technique [17,30,38], one derives the momentum

dependence of the static magnetic susceptibility function,

$$\chi(\mathbf{q}) = -T^2 \sum_l R_l(\mathbf{q}) \left[2 - \frac{1}{2} \sum_{\alpha\sigma\sigma'} \frac{\sigma\gamma_{\alpha s}(\mathbf{q})}{S_{l\sigma} Z_\sigma^{\alpha s}(i\omega_l)} \right]. \quad (8)$$

Here $R_l^{-1}(\mathbf{q}) = [\chi_0(\mathbf{q}, i\omega_l)]^{-1} + \sum_\sigma [G_\sigma^{-2}(i\omega_l) - S_{l\sigma}^{-1}]/2$ with $\chi_0(\mathbf{q}, i\omega_l) = \sum_{\mathbf{k}, \sigma} G_\sigma(\mathbf{k} + \mathbf{q}, i\omega_l) G_\sigma(\mathbf{k}, i\omega_l)/2$ is the bare particle-hole susceptibility. The $\gamma_{\alpha s}(\mathbf{q})$ term in Eq. (8) can be determined from a matrix identity,

$$\sum_{\alpha' s'} \Pi_{\alpha s, \alpha' s'}(\mathbf{q}) \gamma_{\alpha' s'}(\mathbf{q}) = \Omega_{\alpha s}(\mathbf{q}), \quad (9)$$

where

$$\begin{aligned} \Pi_{\alpha s, \alpha' s'}(\mathbf{q}) &= \delta_{\alpha\alpha'} \delta_{ss'} - \sum_{l\sigma} \frac{\Lambda_{\alpha s} \Gamma_\sigma^{\alpha s}(i\omega_l)}{S_{l\sigma} Z_\sigma^{\alpha s}(i\omega_l)} \\ &\quad - \frac{1}{2} \sum_{l\sigma\sigma'} \frac{R_l(\mathbf{q}) \Lambda_{\alpha s} \Gamma_\sigma^{\alpha s}(i\omega_l)}{S_{l\sigma} S_{l\sigma'} Z_\sigma^{\alpha s}(i\omega_l)} \sigma\sigma', \\ \Omega_{\alpha s}(\mathbf{q}) &= -2 \sum_{l\sigma} \frac{R_l(\mathbf{q}) \Lambda_{\alpha s} \Gamma_\sigma^{\alpha s}(i\omega_l)}{S_{l\sigma}} \sigma. \end{aligned} \quad (10)$$

Here the definitions $\Gamma_\sigma^{\alpha s}(i\omega_l) = Z_\sigma^{\alpha s}(i\omega_l)^{-1} - G_\sigma(i\omega_l)$ and $S_{l\sigma} = \sum_{\alpha s} \Lambda_{\alpha s} / [Z_\sigma^{\alpha s}(i\omega_l)]^2$ have been used. Once the local Green function is solved by the DMFT, the \mathbf{q} -dependent static magnetic susceptibility function $\chi(\mathbf{q})$ is fully determined. Divergence of $\chi(\mathbf{q})$ indicates the instability of the PM state. The momentum dependence of $\chi(\mathbf{q})$ affects only the bare susceptibility $\chi_0(\mathbf{q}, i\omega_l)$. In the infinite-dimensional limit ($d \rightarrow \infty$), the \mathbf{q} dependence of $\chi_0(\mathbf{q}, i\omega_l)$ is summarized in a single parameter $X = \sum_i \cos q_i/d$ [23,26],

$$\begin{aligned} \chi_0(\mathbf{q}, i\omega_l) &\equiv \chi_0(X, i\omega_l) \\ &= \frac{-1}{\sqrt{1-X^2}} \int \frac{d\epsilon \rho(\epsilon)}{z - \epsilon} F\left(\frac{z - X\epsilon}{\sqrt{1-X^2}}\right), \end{aligned} \quad (11)$$

where $F(z) = \int d\epsilon \rho(\epsilon)/(z - \epsilon)$ is the Hilbert transform of the noninteracting density of states, with $z = i\omega_l + \mu - \Sigma(i\omega_l)$. The instability of the PM state is addressed depending on a certain value of X that the susceptibility $\chi(X)$ diverges. If $\chi(X)$ diverges at $X = -1$ [or the zone-boundary point $\mathbf{q} = (\pi, \pi, \dots, \pi)$], the PM-AFM transition happens, whereas a divergence of $\chi(X)$ at $X = 1$ (or the uniform zone-center point $\mathbf{q} = \mathbf{0}$) indicates the FM stability against the PM state. Discussions of the PM-FM and the PM-AFM transitions in the signatures of the static magnetic susceptibility function in the aspect are widely available in the literature [25,28,39].

III. NUMERICAL RESULTS

To discuss the magnetic instability of the system, first of all we examine the signature of the static magnetic susceptibility function, χ . Figure 1 shows $\chi(X)$ at some temperatures T with $J = 3$, $U = 0.5$, and $x = 0.1$ for two different values of carrier density n ($n = 0.1$ and 0.097). Here the carrier density is defined as $n = n_\uparrow + n_\downarrow$, $n_\sigma = -\int d\omega \text{Im} G_\sigma(\omega) f(\omega)/\pi$, where $f(\omega) = 1/(1 + e^{\omega/T})$ is the Fermi-Dirac distribution function. Note here that, in DMSs, the hole density can be varied independently on the nominal magnetic doping, for instance Mn replacing the Ga position. Indeed, the hole density

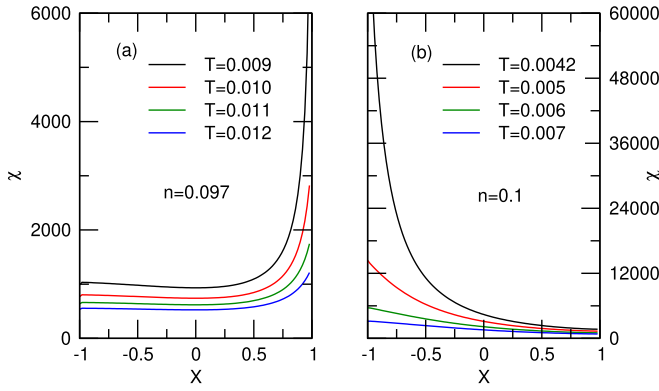


FIG. 1. Static magnetic susceptibility depending on X at different temperatures for $J = 3$, $U = 0.5$, and $x = 0.1$ at $n = 0.097$ (left) and $n = 0.1$ (right).

can be adjusted by nonmagnetic donors or acceptors. The hole density n can thus be equal to the density of the magnetic ions x , or the impurity band can be filled. Moreover, experimental results also reveal that the number of magnetic atoms mediating the magnetic state, the so-called active magnetic ions, is lower than the number of nominal magnetic ones. The situation with one itinerant carrier per active magnetic ion or less (corresponding to the completely or nearly filled impurity band) can still be the factual situation in some samples [6,7]. Once the impurity band is not fully filled, $n = 0.097$ for instance, Fig. 1(a) shows that the magnetic susceptibility function rapidly increases at $X = 1$ as temperature is lowered. If the temperature is sufficiently small, the susceptibility function diverges, indicating the stability of the FM state. In contrast, the magnetic susceptibility function is found to diverge at $X = -1$ in the case of the completely filled impurity band, i.e., at $n = 0.1$ [cf. Fig. 1(b)]. This divergence otherwise indicates the stability of the AFM phase at low temperature.

From the signature of the magnetic susceptibility above, one might establish a diagram of the complex magnetic phase transition when the impurity band is completely filled or nearly filled. The critical temperature of the magnetic phase transition is determined by a divergence of the static susceptibility function. Figure 2 shows us the magnetic phase diagram in the T - n plane at different values of magnetic coupling J for $U = 0.5$ and $x = 0.1$. When the magnetic coupling is small, the impurity band is not clearly split from the main band [7,17], and one finds only the FM phase that is formed due to the delocalization of the itinerant carriers [Fig. 2(a)]. When the magnetic coupling is large enough [Figs. 2(b)–2(d)], the situation is changed because the impurity band induced by the large magnetic coupling is completely separated from the main band [7,17]. Here one finds the AFM state around $n = 0.1$. In this regime, the magnetic coupling is sufficient to lower the FM state in comparison to the AFM one. No low-energy hopping processes, therefore, are allowed in the FM state, whereas in the AFM state hopping is allowed. As a result, the ground state of the system is AFM [7]. Deviating from $n = 0.1$, the FM state emerges. Both FM and AFM transition temperatures increase when increasing the magnetic coupling. For large J , one might find a magnetic phase separation around the point of overlap between AFM and FM states.

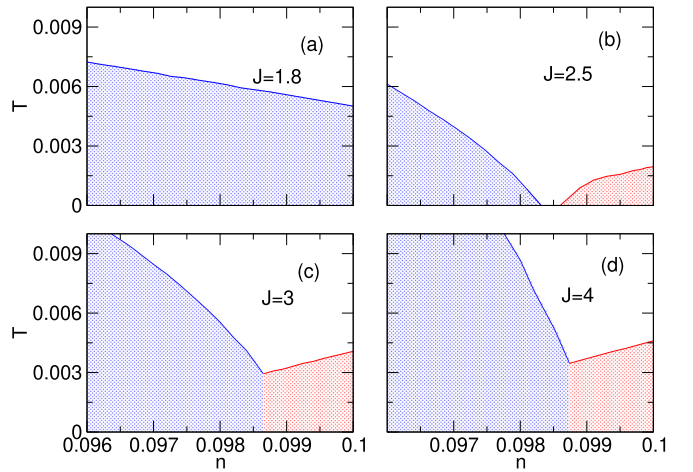


FIG. 2. Magnetic phase diagram in the T - n plane at different values of magnetic coupling J for $U = 0.5$ and $x = 0.1$. The FM state is indicated by blue, while the AFM state is indicated by red.

Note here that the range of J used is relevant to almost DMSs [40], especially for the GaN host semiconductor doped with 5% Mn and Co where the AFM stability has been observed [14].

Note here that, in the present work, although the temporal quantum fluctuations have been fully taken into account in the framework of the DMFT, the spatial fluctuations that might also affect the critical temperature are ignored in the infinite-dimensional approximation. The spatial fluctuations might be considered if the calculation is extended to the site-dependent DMFT, the so-called cluster DMFT [41]. By including the spatial fluctuations, we expect that the critical temperatures would fall very slowly with cluster size, and it would be reduced to 30% for the number of cluster sizes $N_c = 36$ [41,42].

To discuss in more detail the magnetic phase structure when the impurity band is fully filled, in Fig. 3 we analyze the phase diagram in the T - J plane for different U at $n = x = 0.1$.

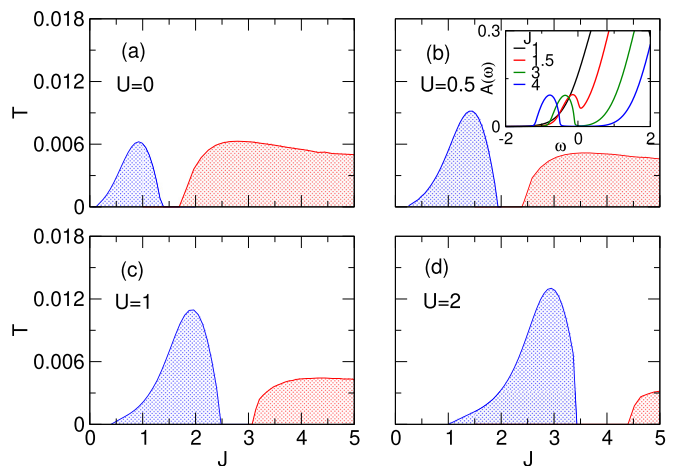


FIG. 3. Magnetic phase diagram in the T - J plane at different disorder potential U for $n = x = 0.1$. The FM state is indicated by blue, while the AFM state is indicated by red. The inset of panel (b) shows the density of states of the itinerant carriers $A(\omega)$ for some values of J at $T = 0$, $U = 0.5$, and $n = x = 0.1$.

As a function of the magnetic coupling J , one always finds two distinct FM and AFM islands. At low J , one finds the FM state, whereas the AFM state stabilizes once J is large. The inset of Fig. 3(b) displays the total density of states of the itinerant carriers $A(\omega) = -\sum_{\sigma} \text{Im}G_{\sigma}(\omega)/\pi$ for ω around the Fermi level with some values of J at $T = 0$, $U = 0.5$, and $n = x = 0.1$. It shows us that at small J ($J < 2$), the impurity band is either not formed or not clearly formed. However, once J is large enough, for instance at $J = 3$, the impurity band is clearly formed and the Fermi level is in a gap opened between the impurity band and the main band, the impurity band is thus completely filled. In this sense, one can believe that, at small J , the system favors the FM state due to the delocalization of the itinerant carriers. Its transition temperature increases when increasing the magnetic coupling. However, once the magnetic coupling is sufficiently large that the impurity band is explicitly formed, the delocalization energy in the impurity band is diminished, leading to a depletion of the FM stability. On the other hand, in this regime the AFM state hopping is allowed. Enlarging the magnetic coupling, therefore, develops the AFM regime. Moreover, the magnetic potential of the majority-spin carriers is suppressed by taking into account the disorder. Increasing the magnetic coupling is needed to compensate for the development of the disorder. The FM and AFM regimes thus shift to the left when increasing the disorder strength. Note here that the magnetic ordering in the fully filled case is strongly dependent on perfect nesting, which is suppressed by the disorder [23,33]. At a given large J value, Fig. 3 shows us that increasing the disorder causes a strong reduction of the AFM-PM transition temperature.

To discuss the characteristics of the magnetic phase transitions in filled impurity band DMSs, we analyze electronic Raman scattering in the PM phase at $n = x$. The imaginary part of the nonresonant Raman response B_{1g} channel can be evaluated from the results of the DMFT via

$$I(\omega) = \pi \int d\nu \int d\varepsilon \rho(\varepsilon) [f(\nu) - f(\nu + \omega)] \times A(\varepsilon, \nu) A(\varepsilon, \nu + \omega), \quad (12)$$

where $A(\varepsilon, \nu) = -\text{Im}[\nu - \varepsilon + \mu - \Sigma(\nu)]^{-1}/\pi$ is the spectral function of the itinerant carriers [43,44].

Figure 4(a) displays $I(\omega)$ for some values of the magnetic coupling J at $U = 0.5$ and $n = x = 0.1$. When the magnetic coupling is small (black line), the ground state of the system is in nonmagnetic order [cf. Fig. 3(b)], and the electronic Raman spectrum exhibits a diffusional response, which is typically observed for single-particle excitations in degenerate or doped semiconductors (for instance, in n -type Si) [45], and is well described by a simple relaxational scattering response [16]. However, when increasing the magnetic coupling, a peak appears at a finite frequency, and the spin fluctuations thus become important with the formation of the SRMO so called magnetic polarons in the PM state. That signature of $I(\omega)$ reveals the formation of the FM long-range order ground state

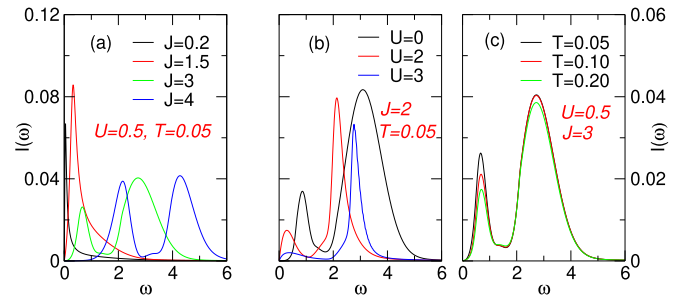


FIG. 4. Imaginary part of the nonresonant Raman response B_{1g} channel $I(\omega)$ at $x = n = 0.1$ for some given values of J at $U = 0.5$, $T = 0.05$ (a), some values of U at $J = 2$, $T = 0.05$ (b), and some values of T at $J = 3$, $U = 0.5$ (c).

[see the blue regime in Fig. 3(b)]. For large magnetic coupling, one finds a two-peak structure in the Raman spectrum. A low-frequency peak identifies the SWLE arising from the impurity band. In this situation, the well-developed AFM long-range order at zero temperature induces a sharp peak in $I(\omega)$ [cf. the red regime in Fig. 3(b)]. Increasing the disorder reduces the magnetic correlations, and the low-frequency peak thus shifts down with a broadening and reduction of the Raman scattering intensity [see Fig. 4(b)]. That feature is similar if one increases temperature, indicating that in the presence of thermal fluctuations, the magnetic polaron and also the spin fluctuations are depressed [cf. Fig. 4(c)].

IV. CONCLUSION

In conclusion, we have studied the nature of the magnetic properties in a nearly or fully filled impurity band diluted magnetic semiconductor described by the Kondo lattice model involving local disorder in assuming that the active magnetic ions in the system are distributed homogeneously. In the framework of dynamical mean-field theory, the static magnetic susceptibility function and the B_{1g} channel Raman response of the microscopic model have been evaluated to survey the magnetic signatures in the system. At low temperatures, when the impurity band is fully or nearly filled, one finds the antiferromagnetic stability against the ferromagnetic state. Moreover, signatures of the B_{1g} channel Raman spectrum show us that the spin dynamics properties with the competition of the short-range magnetic order and short-wavelength excitation might exist in the paramagnetic state of the diluted magnetic semiconductors. Further simulation or experiment considering the problem would be a worthwhile goal of forthcoming studies.

ACKNOWLEDGMENTS

This research is funded by the Vietnam National Foundation for Science and Technology Development (NAFOSTED) under Grant No. 103.01-2019.306.

[1] T. Jungwirth, J. Wunderlich, V. Novák, K. Olejník, B. L. Gallagher, R. P. Campion, K. W. Edmonds, A. W. Rushforth, A. J. Ferguson, and P. Němec, *Rev. Mod. Phys.* **86**, 855 (2014).

[2] T. Dietl and H. Ohno, *Rev. Mod. Phys.* **86**, 187 (2014).

[3] O. M. Fedorych, E. M. Hankiewicz, Z. Wilamowski, and J. Sadowski, *Phys. Rev. B* **66**, 045201 (2002).

- [4] T. Dietl, H. Ohno, F. Matsukura, J. Cibert, and D. Ferrand, *Science* **287**, 1019 (2000).
- [5] T. Dietl, *Nat. Mater.* **9**, 965 (2010).
- [6] T. Jungwirth, J. Sinova, J. Mašek, J. Kurmancupcarera, and A. H. MacDonald, *Rev. Mod. Phys.* **78**, 809 (2006).
- [7] A. Chattopadhyay, S. Das Sarma, and A. J. Millis, *Phys. Rev. Lett.* **87**, 227202 (2001).
- [8] E. H. Hwang and S. Das Sarma, *Phys. Rev. B* **72**, 035210 (2005).
- [9] J. Kienert and W. Nolting, *Phys. Rev. B* **73**, 224405 (2006).
- [10] J. L. Alonso, L. A. Fernández, F. Guinea, V. Laliena, and V. Martín-Mayor, *Nucl. Phys. B* **596**, 587 (2001).
- [11] H. Akai, *Phys. Rev. Lett.* **81**, 3002 (1998).
- [12] A. Kaminski and S. Das Sarma, *Phys. Rev. B* **68**, 235210 (2003); S. Das Sarma, E. H. Hwang, and A. Kaminski, *ibid.* **67**, 155201 (2003); V. M. Galitski, A. Kaminski, and S. Das Sarma, *Phys. Rev. Lett.* **92**, 177203 (2004); A. Kaminski, V. M. Galitski, and S. Das Sarma, *Phys. Rev. B* **70**, 115216 (2004).
- [13] V. Baltz, A. Manchon, M. Tsoi, T. Moriyama, T. Ono, and Y. Tserkovnyak, *Rev. Mod. Phys.* **90**, 015005 (2018).
- [14] J. P. T. Santos, M. Marques, L. K. Teles, and L. G. Ferreira, *Phys. Rev. B* **81**, 115209 (2010).
- [15] M. Gryglas-Borysiewicz, A. Kwiatkowski, P. Juszyński, Z. Ogorzałek, K. Puźniak, M. Tokarczyk, G. Kowalski, M. Baj, D. Wasik, N. Gonzalez Szwacki *et al.*, *Phys. Rev. B* **101**, 054413 (2020).
- [16] P. Nyhus, S. Yoon, M. Kauffman, S. L. Cooper, Z. Fisk, and J. Sarrao, *Phys. Rev. B* **56**, 2717 (1997).
- [17] D.-H. Bui, Q.-H. Ninh, H.-N. Nguyen, and V.-N. Phan, *Phys. Rev. B* **99**, 045123 (2019).
- [18] K. B. Lyons, P. A. Fleury, J. P. Remeika, A. S. Cooper, and T. J. Negran, *Phys. Rev. B* **37**, 2353 (1988).
- [19] P. Prelovšek and J. Jaklič, *Phys. Rev. B* **53**, 15095 (1996).
- [20] H. L. Liu, S. Yoon, S. L. Cooper, S.-W. Cheong, P. D. Han, and D. A. Payne, *Phys. Rev. B* **58**, 10115(R) (1998); S. Yoon, H. L. Liu, G. Schollerer, S. L. Cooper, P. D. Han, D. A. Payne, S.-W. Cheong, and Z. Fisk, *ibid.* **58**, 2795 (1998); C. S. Snow, S. L. Cooper, D. P. Young, Z. Fisk, A. Comment, and J.-P. Ansermet, *ibid.* **64**, 174412 (2001).
- [21] M. Nawrocki, R. Planel, G. Fishman, and R. Galazka, *Phys. Rev. Lett.* **46**, 735 (1981).
- [22] T. Dietl and J. Spałek, *Phys. Rev. Lett.* **48**, 355 (1982).
- [23] A. Georges, G. Kotliar, W. Krauth, and M. J. Rozenberg, *Rev. Mod. Phys.* **68**, 13 (1996).
- [24] I. D. Marco, P. Thunström, M. I. Katsnelson, J. Sadowski, K. Karlsson, S. Lebègue, J. Kanski, and O. Eriksson, *Nat. Commun.* **4**, 2645 (2013); G. Kotliar, S. Y. Savrasov, K. Haule, V. S. Oudovenko, O. Parcollet, and C. A. Marianetti, *Rev. Mod. Phys.* **78**, 865 (2006).
- [25] A. Chattopadhyay, A. J. Millis, and S. Das Sarma, *Phys. Rev. B* **61**, 10738 (2000).
- [26] J. K. Freericks and V. Zlatić, *Rev. Mod. Phys.* **75**, 1333 (2003).
- [27] N. Furukawa, *J. Phys. Soc. Jpn.* **63**, 3214 (1994); **64**, 2754 (1995); **65**, 1174 (1996); in *Physics of Manganites*, edited by T. A. Kaplan and S. D. Mahanti (Kluwer, New York, 1999), Fundamental Materials Research, p. 1.
- [28] E. Dagotto, *Nanoscale Phase Separation and Colossal Magnetoresistance: The Physics of Manganites and Related Compounds* (Springer, Heidelberg, 2003).
- [29] K. Kagami, M. Takahashi, and K. Kubo, *J. Supercond.* **18**, 121 (2005); K. Kagami, M. Takahashi, C. Yasuda, and K. Kubo, *Sci. Technol. Adv. Mater.* **7**, 31 (2006); M. Takahashi, *Materials* **3**, 3740 (2010).
- [30] V.-N. Phan and M.-T. Tran, *Phys. Rev. B* **72**, 214418 (2005).
- [31] F. Zhong, J. Dong, and Z. D. Wang, *Phys. Rev. B* **58**, 15310 (1998).
- [32] B. M. Letfulov and J. K. Freericks, *Phys. Rev. B* **64**, 174409 (2001).
- [33] V. Janiš and D. Vollhardt, *Int. J. Mod. Phys. B* **6**, 731 (1992); R. Vlaming and D. Vollhardt, *Phys. Rev. B* **45**, 4637 (1992); V. Janiš, M. Ulmke, and D. Vollhardt, *Europhys. Lett.* **24**, 287 (1993).
- [34] M. Mayr, G. Alvarez, and E. Dagotto, *Phys. Rev. B* **65**, 241202(R) (2002).
- [35] M. P. Kennett, M. Berciu, and R. N. Bhatt, *Phys. Rev. B* **66**, 045207 (2002).
- [36] B. Michaelis and A. J. Millis, *Phys. Rev. B* **68**, 115111 (2003).
- [37] U. Brandt and C. Mielsch, *Z. Phys. B* **75**, 365 (1986).
- [38] T. Minh-Tien, *Phys. Rev. B* **67**, 144404 (2003).
- [39] A. Chattopadhyay, A. J. Millis, and S. Das Sarma, *Phys. Rev. B* **64**, 012416 (2001); *Lecture Notes on Electron Correlations and Magnetism* (World Scientific, Singapore, 1999).
- [40] Y. Yildirim, Ph.D. thesis, Florida State University (2007); M. Abolfath, T. Jungwirth, J. Brum, and A. H. MacDonald, *Phys. Rev. B* **63**, 054418 (2001); J. Okabayashi, A. Kimura, O. Rader, T. Mizokawa, A. Fujimori, T. Hayashi, and M. Tanaka, *ibid.* **58**, R4211 (1998); F. Matsukura, H. Ohno, A. Shen, and Y. Sugawara, *ibid.* **57**, R2037 (1998).
- [41] T. A. Maier, M. Jarrell, T. Prushke, and M. Hettler, *Rev. Mod. Phys.* **77**, 1027 (2005).
- [42] M. Jarrell, T. Maier, C. Huscroft, and S. Moukouri, *Phys. Rev. B* **64**, 195130 (2001).
- [43] J. K. Freericks, T. P. Devereaux, and R. Bulla, *Phys. Rev. B* **64**, 233114 (2001).
- [44] J. K. Freericks and T. P. Devereaux, *Phys. Rev. B* **64**, 125110 (2001).
- [45] P. Leroux-Hugon, *Phys. Rev. Lett.* **29**, 939 (1972).